


Augmented Production of Platelets From Cord Blood With Euchromatic Histone Lysine Methyltransferase Inhibition

Yiying Liu^{1,2}, Jingjing Zhao^{1,2}, Yan Wang^{3,4}, Pei Su^{1,2}, Hongtao Wang^{1,2}, Cuicui Liu^{1,2,*},
Jiaxi Zhou^{1,2,*} 

¹State Key Laboratory of Experimental Hematology, National Clinical Research Center for Blood Diseases, Haihe Laboratory of Cell Ecosystem, Institute of Hematology and Blood Diseases Hospital, Chinese Academy of Medical Sciences and Peking Union Medical College, Tianjin, People's Republic of China

²Center for Stem Cell Medicine, Chinese Academy of Medical Sciences and Department of Stem Cells and Regenerative Medicine, Peking Union Medical College, Tianjin, People's Republic of China

³State Key Laboratory of Molecular Oncology, National Cancer Center/National Clinical Research Center for Cancer/Cancer Hospital, Chinese Academy of Medical Sciences and Peking Union Medical College, Beijing, People's Republic of China

⁴Tianjin Medical University, Tianjin, People's Republic of China

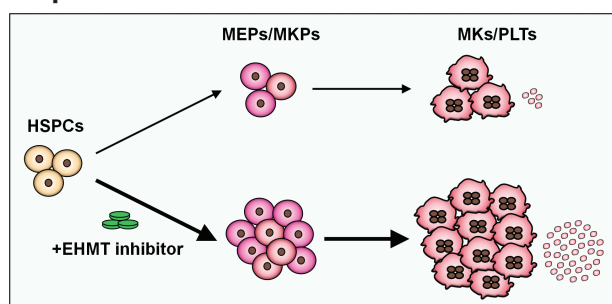
*Corresponding author: Cuicui Liu, State Key Laboratory of Experimental Hematology, National Clinical Research Center for Blood Diseases, Haihe Laboratory of Cell Ecosystem, Institute of Hematology and Blood Diseases Hospital, Chinese Academy of Medical Sciences and Peking Union Medical College, Tianjin 300020, People's Republic of China. Email: liucuicui@ihcams.ac.cn; or, Jiaxi Zhou, State Key Laboratory of Experimental Hematology, National Clinical Research Center for Blood Diseases, Haihe Laboratory of Cell Ecosystem, Institute of Hematology and Blood Diseases Hospital, Chinese Academy of Medical Sciences and Peking Union Medical College, Tianjin 300020, People's Republic of China. Email: zhoujx@ihcams.ac.cn

Abstract

Cord blood hematopoietic stem/progenitor cells (CB-HSPCs) have emerged as a promising supply for functional platelets to potentially alleviate the increasing demand for platelet transfusions, but the clinical application has been limited by the undefined molecular mechanism and insufficient platelet production. Here, we performed single-cell profiling of more than 16 160 cells to construct a dynamic molecular landscape of human megakaryopoiesis from CB-HSPCs, enabling us to uncover, for the first time, cellular heterogeneity and unique features of neonatal megakaryocytes (MKs) and to also offer unique resources for the scientific community. By using this model, we defined the genetic programs underlying the differentiation process from megakaryocyte-erythroid progenitors (MEPs) to MKs via megakaryocyte progenitors (MKPs) and identified inhibitors of euchromatic histone lysine methyltransferase (EHMT), which, when applied at the early stage of differentiation, significantly increase the final platelet production. At the mechanistic level, we found that EHMT inhibitors act to selectively induce the expansion of MEPs and MKPs. Together, we uncover new mechanistic insights into human megakaryopoiesis and provide a novel chemical strategy for future large-scale generation and clinical applications of platelets.

Key words: platelet production; cord blood; EHMT inhibitors; MEP.

Graphical Abstract



Significance Statement

In this study, we reveal, for the first time, the transcriptional landscape of human megakaryopoiesis from cord blood and identify euchromatic histone lysine methyltransferase inhibitors as powerful tools for substantial improvement of platelet production. This work provides novel insights into human neonatal megakaryopoiesis and new tools for future large-scale generation and clinical applications of platelets.

Received: 10 December 2021; Accepted: 5 June 2022.

© The Author(s) 2022. Published by Oxford University Press.

This is an Open Access article distributed under the terms of the Creative Commons Attribution-NonCommercial License (<https://creativecommons.org/licenses/by-nc/4.0/>), which permits non-commercial re-use, distribution, and reproduction in any medium, provided the original work is properly cited. For commercial re-use, please contact journals.permissions@oup.com.

Introduction

Platelets are anucleate cytoplasmic discs derived from megakaryocytes (MKs) and play essential roles in hemostasis, thrombosis, angiogenesis, and immune regulation.¹ The transfusion of allogeneic platelets is needed for a range of patients with severe thrombocytopenia, platelet functional defects, or undergoing surgery.² However, current platelet transfusion is completely donor dependent, which leads to a limited supply for clinical therapy.³ The growing demand for platelets is also severely limited by the high cost, short shelf life, and high risk for transfusion complications such as bacterial contamination, transfusion-related acute lung injury, allergic transfusion reactions, febrile nonhemolytic transfusion reactions, and disease transmission.^{4,5} The limited blood supply and safety challenges have impelled the community to create new sources for platelets.

Evidence is accumulating that the generation of MKs and platelets can commerce with human hematopoietic stem/progenitor cells (HSPCs) *in vitro*.⁶ The availability of stem cells from cord blood (CB), the relatively defined differentiation process, and the massive efforts of developing induction methods have made the generation of platelets *in vitro* from cord blood hematopoietic stem/progenitor cells (CB-HSPCs), a highly promising approach for clinical applications,⁷ while efforts have been made by us and others to use this system for optimizing platelet production and quality.^{8,9} However, the quantity of platelet production is still limited and must be further improved, probably through more detailed exploration of the molecular program underlying human neonatal megakaryopoiesis and systematic optimization to reduce the cost and improve efficiency to ultimately meet clinical requirements.

Single-cell sequencing ushers in a golden age for many research fields including the study of megakaryopoiesis, allowing us to decipher the molecular features and cellular heterogeneity of both human embryonic and adult MKs *in vivo* at a single-cell resolution.^{10,11} To gain insights into the process of human megakaryopoiesis, we further modeled human embryonic and adult megakaryopoiesis *in vitro* and characterized the gene expression programs dictating megakaryocytic differentiation from human embryonic stem cells (hESCs) and adult bone marrow (BM) for the first time.^{10,11} These new findings have broadened our knowledge of the functional diversity and ontogenic signatures of MKs at different developmental stages. However, the transcriptional features of neonatal MKs derived from CB-HSPCs and the molecular signatures underlying MK differentiation are still undefined and need to be investigated.

In this study, we conducted single-cell sequencing using the CB-HSPC system and provided the first single-cell transcriptomic landscape of human neonatal megakaryopoiesis from CB-HSPCs. We unveiled the dynamics of cell populations and the unique features of neonatal MKs compared with their embryonic and adult counterparts and uncovered the molecular dynamics of the developmental trajectory from MEPs to MKs via MKPs. By applying a small-scale screening of chemical compounds, we identified the inhibitors of euchromatic histone lysine methyltransferase (EHMT) as strong inducers for MEP proliferation, MK specification, and subsequent platelet generation. The cost-effective strategy based on chemical approaches represents an

important step toward the large-scale production of platelets for future clinical applications.

Methods

Human Megakaryocytic Differentiation From CB-CD34⁺ Cells

CB samples were collected from healthy neonates umbilical cord with the informed consent of their parents, under the awareness and approval of the ethics committee of Hematology and Blood Diseases Hospital, Medical Sciences Academy of China. The isolation of CD34⁺ cells and megakaryocytic induction were performed as previously described.⁸ Briefly, CD34⁺ cells (cell density, 1×10^5 cells/mL) enriched with magnetic beads were first cultured in serum-free medium (StemSpan SFEM; Stem Cell Technologies) containing 1% penicillin/streptomycin, TPO (50 ng/mL), SCF (20 ng/mL), and IL-3 (20 ng/mL) for 6 days. Then, the cells (cell density, 5×10^5 cells/mL) were cultured in StemSpan medium supplemented with TPO (50 ng/mL) and IL-11 (20 ng/mL) for the next 9 days. The medium was replaced with fresh medium every 3 days. The chemical compounds were dissolved in dimethyl sulfoxide (DMSO, Sigma-Aldrich) and added into the cultures with a concentration of 200 nM.

Sample Collection and Single-Cell RNA-Seq

To investigate human neonatal megakaryopoiesis, we collected total cells at days 4, 8, and 12 of MK differentiation and performed the single-cell RNA-Seq using 10x Genomics Chromium platform (Novogene). Briefly, the cells with more than 95% viability were resuspended in PBS buffer containing 1% BSA at the density of 1×10^6 /mL and subjected to 10x Genomics Chromium Controller to generate Gel Beads-in-Emulsion. mRNAs were released by lysed cells and recovered to cDNA after RT-PCR. cDNAs were mixed with barcoded oligonucleotides inside the droplets. The RNA-Seq libraries of single cells were established by 10x_Single_cell_RNA-seq 3 library Kit V2, and sequencing on Illumina_NovaSeq_5000 with pair-end 150 bp was performed (Novogene). Cells with or without UNC0631 treatment were collected on day 9 of MK differentiation. The same procedure for 10x Genomics single-cell RNA-Seq (Novogene) was performed using 10x_Single_cell_RNA-seq 3 library Kit V3. All the data were deposited at National Omics Data Encyclopedia with accession numbers OEP003290 and OEP002903. The single-cell data of MKs from hESCs and BM models (accession numbers GSE144024 and OEP000756, respectively), which published in our previous study,^{10,11} were introduced and re-analyzed for comparison with CB-derived MKs.

Data Preprocessing and Quality Control

The 10x Genomics clean data were aligned and quantified using the Cell Ranger count pipeline 2.1.0 with GRCh38 human reference genome by STAR (<http://www.10xgenomics.com>). We used Python-based Scrublet software (version 0.2.1) to remove doublet for each data set with recommended parameters based on the doublet score density for observed transcriptomes and simulated doublets. Cells with 200-6000 genes were retained in the initial quality control, and then cells with >20% of mitochondrial gene expression were excluded. Sixteen thousand one hundred and sixty cells in all 3 samples during neonatal

megakaryopoiesis and 21 664 cells treated with DMSO or UNC0631 passed the quality control and were used for further analysis.

Cell Clustering and Dimensionality Reduction

We used Seurat package (version 3.2.0) to perform downstream analysis and visualization after quality control was completed. For all 3 samples during neonatal megakaryopoiesis, we merged them then normalized sequencing data by using the default function “NormalizeData” with scale factor 10 000 and calculated top 2000 high-variable genes (HVG) by using function “FindVariableFeatures.” We conducted principal component analysis based on the expression matrix of RNA-slot features and the selected top 15 significant PCs for dimensionality reduction and clustering. Afterward, we identified cell clusters using the “FindNeighbors”, “FindClusters” and “RunUMAP” with Uniform Manifold Approximation and Projection (UMAP; resolution = 0.1).

Cell Label Transfer

The single-cell data of cells treated with DMSO or UNC0631 were, respectively, normalized and identified top 2000 HVGs by function “NormalizeData” and “FindVariableFeatures” in Seurat. Function “SelectIntegrationFeatures” was used to integrate HVGs from DMSO and UNC0631. Function “ScaleData” and “RunPCA” were carried out with integrated HVGs in DMSO and UNC0631, respectively. Then, these 2 data were integrated by using “FindIntegrationAnchors” and “IntegrateData” function to remove batch effects. To annotate cell types of integrated single cells, we transferred cell-type annotation that identified in all 3 samples during neonatal megakaryopoiesis by using “FindTransferAnchors” and “TransferData” function with default parameters. The top 30 PCs calculated after integration were used to visualize different clusters by UMAP.

Identification and Analysis of Differentially Expressed Genes

We used Seurat “FindAllMarkers” to compare different clusters and find differentially expressed genes. Gene ontology (GO) enrichment was performed by using DAVID and g:Profiler (<https://biit.cs.ut.ee/gprofiler/>). Gene sets enrichment analysis was performed using version 6.2.

The Relationships Between MKs Derived From Different Sources

The single-cell data of MKs derived from BM and hESC were from our earlier studies.^{10,11} We merged these 3 data sets and used Seurat “FindAllMarkers” to compare different clusters and find differentially expressed genes. Pearson correlation coefficient was calculated by cor function in R (version 3.5.3). The correlation analyses of MK mature gene expression were performed using GraphPad Prism 8 (version 8.0.2).

Gene Set Score

Gene set score was calculated by using AddModuleScore with “ctl=5” in Seurat. Gene sets were downloaded from MSigDB (version 6.2).

Trajectory Inference

We used Monocle (v2.10.1) to conduct pseudotime analysis to calculate the potential differentiation trajectory, while pseudo-object was built by using “newCellDataSet” function. MEP/MKP/MK marker genes were selected with function setOrderingFilter to estimate pseudotime. To examine the module cluster with pseudotime, different genes were calculated by “differentialGeneTest” function with MEP/MKP/MK marker genes. Genes with $qval < 0.001$ were assigned on differentially expressed genes (DEGs) between each module. “plot_cell_trajectory” and “plot_pseudotime_heatmap” functions were utilized for visualization.

Flow Cytometry Analysis

We analyzed the percentage and count of MKs and platelets by using Canto II flow cytometer. MKs and platelets at different time points of culture were collected and labeled with APC-CD41a and PE-CD42b antibodies (BD) at room temperature for 30 minutes. The flow cytometry data were analyzed using FlowJo (v10) software.

In Vivo Transplantation Assay

Female NOD/Shi-scid/IL2Rgnull (NOG) mice were purchased from Vital River Laboratory Animal Technology (Beijing, China) and housed with free access to food and water in a specific-pathogen-free condition. All animal protocols were approved by the Animal Care and Use Committee of State Key Laboratory of Experimental Hematology. We irradiated the mice with 2 Gy ray radiation and injected the cells treated with DMSO or UNC0631 after 9 days' culture into the tail vein. We then collected 5 μ L of mouse peripheral blood and labeled it with anti-human and anti-mouse CD41 antibodies at different time points for human platelet analysis using a FACS CantoII flow cytometer (BD).

In Vitro 5-Bromodeoxyuridine Incorporation Assays

5-Bromodeoxyuridine (BrdU) was added into the culture medium (1 mM) for 4 hours, and cells were collected to analyze the BrdU incorporation using the FITC-BrdU Flow kit (BD Pharmingen) following the manufacturer's instructions.

Statistical Analysis

All data were presented as the mean \pm SEM. Statistical analyses were performed using GraphPad Prism software. The Student's *t* test was used for comparing the differences between 2 groups. Differences were considered statistically significant when $P < .05$. Asterisks indicate statistically significant differences ($*P < .05$, $**P < .01$, and $***P < .001$).

Results

Single-Cell Transcriptomic Profiling of Neonatal Megakaryopoiesis From Human CB-CD34⁺ Cells

We have recently unveiled the transcriptomic profile of human embryonic and adult megakaryopoiesis and the cellular heterogeneity of the related MKs.^{10,11} To further explore the dynamics of human neonatal megakaryopoiesis, we induced CD34⁺ HSPCs from neonatal CB to generate MKs and platelets.⁸ To characterize the gene expression programs dictating megakaryocytic differentiation, we

selected high-quality intact single cells at day 4, day 8, and day 12 of megakaryocytic differentiation, respectively, and performed single-cell transcriptomic sequencing using the 10× Genomics Chromium platform (Fig. 1A). As shown by UMAP, we selected 16 160 single cells at all time points for analysis after quality control was completed, with over 2500 genes analyzed in each cell (Fig. 1B, Supplementary Fig. S1A). Six cell populations as featured by the expression of known marker genes^{11,12} were readily recognized and annotated, including MKs, megakaryocyte progenitors (MKPs), megakaryocyte-erythroid progenitors (MEPs), immature myeloid progenitors (iMPs), eosinophil-basophil-mast cell progenitors (EBMPs), and neutrophil progenitors (NeuPs) (Fig. 1B). Among them, the cell clusters in the MK lineage (MEP, MKP, and MK) represented approximately 70% of total cells (Fig. 1C), indicating that this model is viable for the study of human megakaryopoiesis. As expected, the MK cluster showed typical megakaryocytic features, including the highest expression of *ITGB3* (CD61) and *GP1BA* (CD42b) (Fig. 1D) and the enrichment of gene sets related to platelet function (Supplementary Fig. S1B). In addition to the megakaryocytic features, the MKP cluster also exhibited characteristics of the mitotic cell cycle, such as high expression of *UBE2C* (Ubiquitin Conjugating Enzyme E2 C) and *HBD* (Hemoglobin Subunit Delta) (Fig. 1D, Supplementary Fig. S1C). In contrast to MKP, the MEP cluster exhibited stronger proliferative and erythroid characteristics, as characterized by higher expression of *MYC* (MYC Proto-Oncogene) and *KLF1* (Kruppel Like Factor 1) (Fig. 1D, Supplementary Fig. S1C). Thus, human megakaryopoiesis induced from CB-CD34⁺ cells faithfully recapitulates the megakaryocytic differentiation process, as revealed by single-cell transcriptomic analysis.

To further explore the associated molecular features during megakaryocytic differentiation, we dissected the dynamics of cell populations in the MK lineage and found that the MEP population was dominant among the differentiated cells at day 4 and gradually diminished while MK differentiation progressed (Fig. 1E). Furthermore, the genes involved in the DNA replication process and those marking the S phase of the cell cycle were significantly enriched in MEP and MKP populations (Fig. 1F, 1G), indicative of a potential highly proliferative state. To unveil the molecular programs underlying MK differentiation, we performed Monocle analysis, which clearly showed the developmental trajectory from the MEP to MK cluster via MKP (Fig. 1H). We identified 2 different gene expression modules, termed as Module 1 and Module 2, by performing branched expression analysis modeling (Fig. 1I). Many translation-related genes enriched in Module 1 were gradually downregulated upon MK differentiation, while the platelet function-related genes enriched in Module 2 were gradually upregulated on MK differentiation (Fig. 1J). The subsequent analysis of the transcription factor intersection network led us to find that multiple transcription factors regulating the cell cycle progression, such as *E2F2* (E2F Transcription Factor 2), *MYC* (MYC Proto-Oncogene), and several high mobility group proteins, were highly enriched in Module 1 (Fig. 1J). By contrast, more than 20 transcription factors, such as *MEIS1* (Meis Homeobox 1) and *FLI1* (Friend Leukemia Integration 1) that were known to regulate MK maturation,^{13,14} were highly enriched in Module 2 (Fig. 1J).

Together, we produced the transcriptomic profiling of human neonatal megakaryopoiesis at the single-cell resolution, providing a robust database for further investigation.

Comparison Between Neonatal MKs and Embryonic or Adult MKs

Although striking differences have been reported concerning MK ploidy and platelet production efficiency during various developmental stages,¹⁵ the ontogenic details of MKs at the molecular level remain unexplored. By comparing the CB-derived neonatal MKs with our previously reported embryonic or adult MKs,^{10,11} we found that the CB-derived MKs have a stronger correlation with adult-type MKs derived from BM, with weaker similarity with hESC-derived MKs (Fig. 2A). Furthermore, the expression of maturation-related genes¹¹ exhibited a much stronger correlation (0.96) between neonatal and adult MKs and weaker correlation (0.84) between neonatal and embryonic MKs (Fig. 2B), indicating that MKs from CB and BM have similar levels of maturity. Thus, neonatal and adult MKs are common in gene expression and are distinct from embryonic MKs derived from hESCs.

To further determine the developmental differences among MKs in different models, we integrated the transcriptomic data from these in vitro-generated MKs for further analysis. The heatmap of highly DEGs revealed substantial differences among these 3 groups (Fig. 2C). For instance, the hESC-derived MKs displayed a strong tendency toward the expression of hemoglobin genes involved in gas transport (Fig. 2D, 2E), reminiscent of the previous studies that fetal MKs showed a tendency toward “leaky” erythroid gene expression when compared with adult MKs in BM.^{10,15} Despite many common genes, some differences in expression were also observed in MKs from BM and CB (Fig. 2C). Specifically, many genes related to platelet function, such as *vWF*, *CD36*, *CD59*, and *CXCR4* (C-X-C Motif Chemokine Receptor 4), showed the highest expression in adult MKs (Fig. 2D, 2E), probably indicative of a high potential of platelet generation.¹⁶ By contrast, the CB-derived MKs exhibited stronger protein translation characteristics, as suggested by the enrichment of genes related to translational initiation and protein synthesis, such as the translation initiation factor *EIF1AY* (Eukaryotic Translation Initiation Factor 1A Y-Linked) (Fig. 2D, 2E, Supplementary Fig. S2A). Interestingly, despite the unknown functions in MK development, several genes were specifically expressed in CB-derived MKs, such as *MEG3* (Maternally Expressed Gene 3), a long noncoding RNA whose expression is modulated by the uterine environment and dysregulated in many diseases of metabolic dysfunction,¹⁷ indicating a potential distinct function of neonatal MKs.

We recently revealed, unequivocally, the existence of cellular heterogeneity of embryonic and adult MKs both in vivo and in vitro.^{10,11} We, therefore, asked whether heterogeneous subpopulations were also present in neonatal MKs. Based on unsupervised clustering, we partitioned the MKs into 3 distinct clusters, termed hereafter as MK1-MK3 (Supplementary Fig. S2B). Among them, the MK2 subpopulation was characterized by the enrichment of genes regulating platelet function and MK development, such as *TUBB1* (Tubulin Beta 1 Class VI) and *CD9* (Supplementary Fig. S2C). In contrast, genes with immune features, such as *S100A11* (S100 Calcium Binding Protein A11), *MPO* (Myeloperoxidase), and *LYZ* (Lysozyme), were highly expressed in MK3 but not in MK1 or MK2 (Supplementary Fig. S2C). These results demonstrated that neonatal MKs derived from CB were also heterogeneous. The ontogenic differences of MKs were also explored by comparing the MK subpopulations derived from CB with

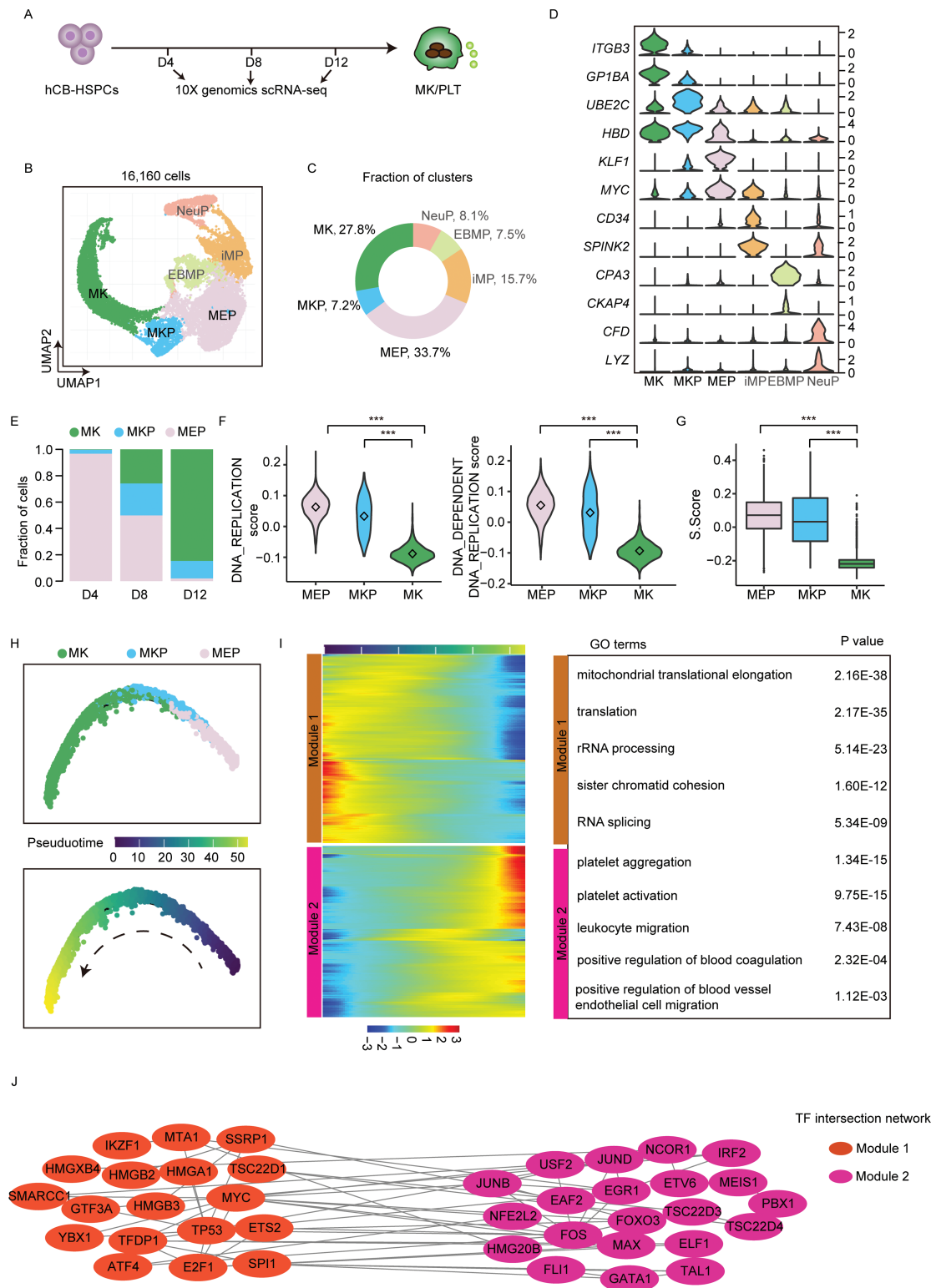


Figure 1. Single-cell transcriptomic profiling of human megakaryopoiesis from CB-CD34⁺ cells. **(A)** Schematic diagram of single-cell RNA-Seq of megakaryopoiesis from CB-CD34⁺ cells at 3 time points. **(B)** Cell clusters of 16 160 single cells visualized by UMAP showing 6 clusters of human MKs from CB-CD34⁺ cells. **(C)** Pie chart showing proportions of the 6 clusters. **(D)** Volin plot shows the marker genes for each cluster. **(E)** Fraction of MKs, MKPs, and MEPs in day 4, day 8, and day 12 of MK differentiation from CB-CD34⁺ cells. **(F)** The score of DNA replication and DNA-dependent DNA replication between MEP, MKP, and MK clusters. Unpaired 2-sided Wilcoxon test, ****P* < .001. **(G)** The score of S stage between MEP, MKP, and MK clusters. Unpaired 2-sided Wilcoxon test, ****P* < .001. **(H)** The trajectory (up) and pseudotime (down) of cell clusters in MK lineage. **(I)** Heatmap showing 2 models with pseudotime (left) and GO enrichment of DEGs between models in the left. **(J)** The intersection network of TF in Fig. 11 based on the string database (<https://string-db.org/>).

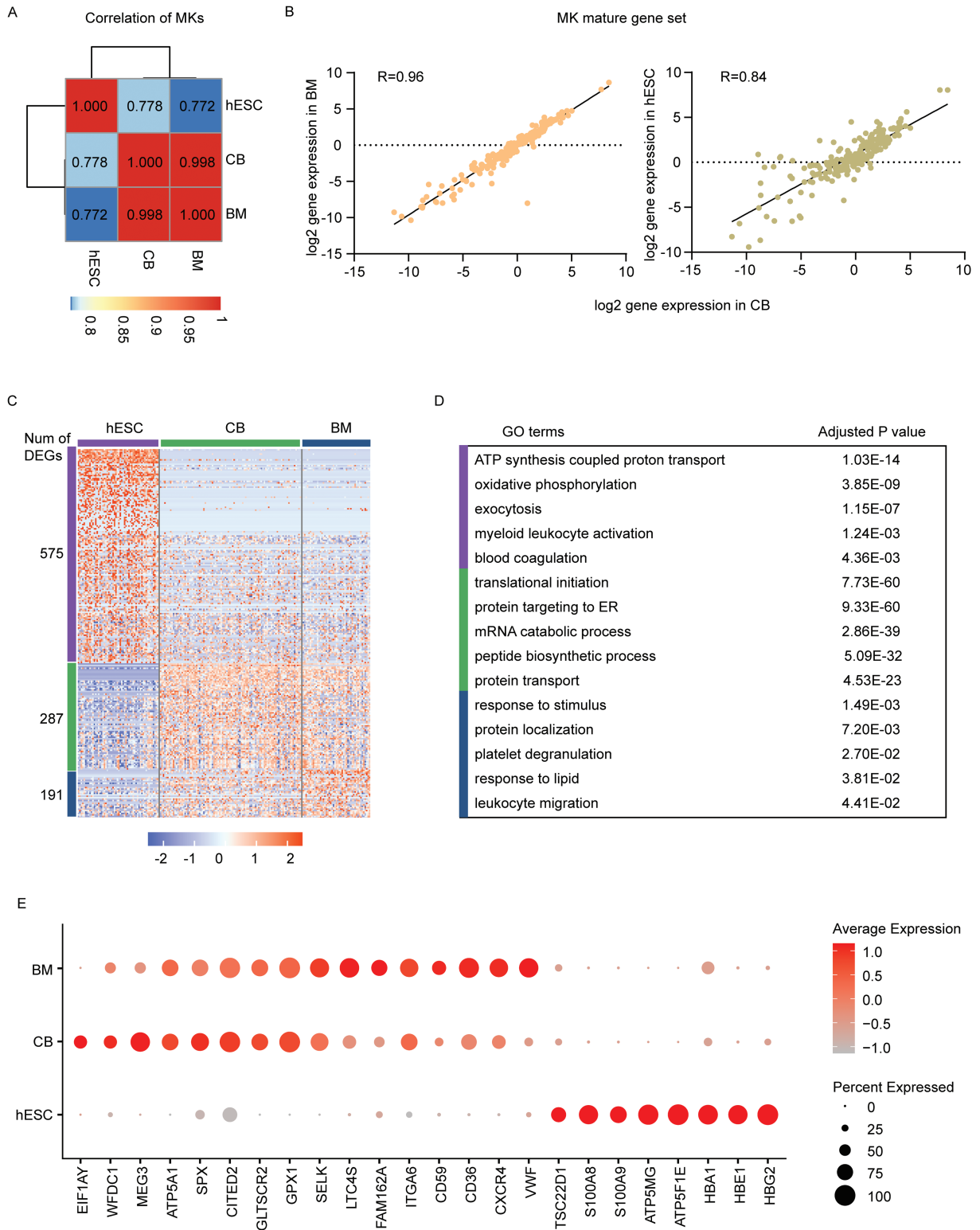


Figure 2. The comparison between CB-derived neonatal MKs and embryonic or adult MKs. **(A)** The correlation of MKs from CB, hESC, and BM. Data of hESC and BM-derived MKs were obtained from previous studies.^{10,11} **(B)** The correlation of mature gene expression between MKs from CB/ BM (left) and CB/hESC (right). **(C)** Heatmap showing the total DEGs between MKs derived from CB, hESC, and BM. **(D)** GO enrichment of DEGs in Fig. 2C. Highlighted GO terms were selected by *P* value (<.05). **(E)** Dot plot showing the gene expression in MKs derived from CB, hESC, and BM. Abbreviations: CB, cord blood; DEGs, differentially expressed genes; DMSO, dimethyl sulfoxide; GO, gene ontology; hESC, human embryonic stem cell; MK, megakaryocyte.

the corresponding subpopulation from hESCs or adult BM, as identified in our previous studies.^{10,11} Interestingly, the genes related with platelet degranulation were much highly expressed in BM-MK2 and CB-MK2 (Supplementary Fig. S2D), probably indicative of a high potential of platelet generation. More importantly, hESC-MK4 exhibited a stronger monocyte/macrophage signature,¹⁰ while CB-MK3 and BM-MK3 showed a stronger neutrophil signature¹⁸ (Supplementary Fig. S2E), consistent with the observation of embryonic and adult MKs in vivo.^{10,11,16}

Thus, the ontogenic changes during human megakaryopoiesis can be well modeled in vitro, and the MKs derived from the CB model exhibit distinct characteristics, providing a potentially powerful tool for platelet regeneration.

EHMT Inhibitors Significantly Promote Platelet Generation

After identifying the molecular features of human neonatal megakaryopoiesis at a single-cell level, we further explored how a large number of platelets might be produced using the CB model. We and others have found that chemical compounds are powerful tools for the efficient generation of platelets.^{8,19} To further improve platelet production, we introduced the epigenetics compound library (TargetMol) and conducted a small-scale screening at the recommended

concentration under conditions supporting megakaryocytic differentiation from CB-CD34⁺ cells (Fig. 3A). Each chemical compound was added from day 3 of differentiation while the production of MKs and platelets was analyzed after 12 days of culture (Fig. 3A, Supplementary Table S1). The screening experiments allowed us to identify UNC0631, A366, UNC0642, and UNC0638, all known as inhibitors of EHMT,^{20,21} which significantly increased the percentage of CD41a⁺CD42b⁺ MKs and subsequent platelets, much superior to other compounds (Fig. 3B, Supplementary Fig. S3A). To determine the optimal concentration, we performed concentration-dependent experiments and found that the effect of EHMT inhibitors on MK generation was the strongest at 200 nM, but weakened above 2 μ M (Supplementary Fig. S3B). To confirm that the outcomes were specific for EHMT inhibition, we further measured the effects of chemical inhibitors on the level of H3K9me2 by flow cytometry. Indeed, the treatment of UNC0631 or A366 decreased the H3K9me2 level, with no significant effect on total expression of histone H3 (Fig. 3C, 3D). We also performed EHMT2 knockdown in CB-CD34⁺ cells (Supplementary Fig. S3C). We found EHMT2 gene depletion also enhanced the MK production (Supplementary Fig. S3D), although the effects is much less significantly than the inhibitors. Likewise, the EHMT2 knockdown also decreased the H3K9me2 level (Supplementary Fig. S3E, S3F). These results indicate the correlation between the

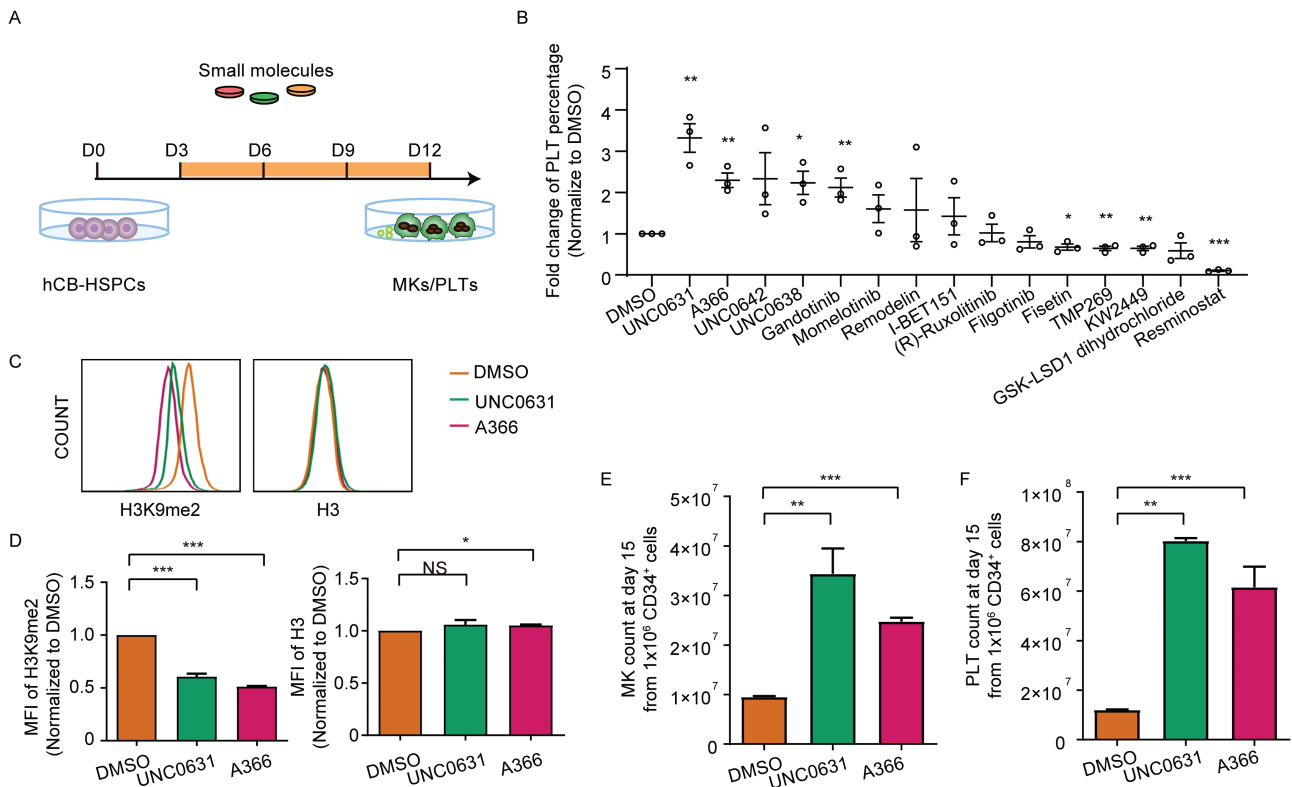


Figure 3. EHMT inhibitors significantly promote platelet generation. **(A)** Schematic diagram of small molecule screening during MK differentiation. The complete list of chemical factors examined was shown in Supplementary Table S1. **(B)** Fold changes of CD41a⁺CD42b⁺ platelet percentage at day 15 with treatment of different small molecules from day 3 ($n = 3$). All values were normalized to the level (= 1) of DMSO. **(C)** Flow cytometry analysis of the expression levels of H3K9me2 and H3 in cells with or without EHMT inhibitor treatment. **(D)** Mean fluorescence intensity (MFI) showing the expression levels of H3K9me2 and H3 in CB-derived cells when treated with UNC0631 or A366 ($n = 3$). All values were normalized to the level (= 1) of DMSO. **(E)** MK count at day 15 generated from seeded 1×10^6 CD34⁺ cells ($n = 3$). **(F)** Platelet count at day 15 generated from seeded 1×10^6 CD34⁺ cells ($n = 3$). Abbreviations: CB, cord blood; EHMT, euchromatic histone lysine methyltransferase; DMSO, dimethyl sulfoxide; MK, megakaryocyte. Student's *t* test, * $P < .05$, ** $P < .01$, and *** $P < .001$.

histone methyltransferase activity and the effects on MK lineage.

We also carefully quantify the change during the whole process. The addition of a single EHMT inhibitor, UNC0631 or A366, could generate $2\text{--}4 \times 10^7$ mature MKs at day 15 induced from 1×10^6 initiating CD34⁺ cells, with an increase over 3-folds than the control group (Fig. 3E). To further assess the yield of platelets, we collected the cultural supernatant for platelet analysis at day 15. Remarkably, the single small molecule led to the production of 6- to 8-fold more total platelets from the equal number of initiating cells (Fig. 3F). As such, we propose that EHMT inhibitors might be used as highly potent tools for future large-scale platelet generation in vitro.

EHMT Inhibitors Exert Their Effects at the Early Proliferation Stage

As described previously by us,⁸ megakaryocytic differentiation from HSPCs goes through a stepwise process including 3 stages: HSPC proliferation (days 0–6), MK differentiation (days 6–9), and platelet generation or release (days 9–15). We then asked at which stage(s) of MK differentiation EHMT inhibitors exert their effects. Among all the stages tested, the treatment of EHMT inhibitors at the early proliferative stage, especially at days 3–6, resulted in the largest enhancement of the final generation of CD41a⁺CD42b⁺ MKs and platelets, even better than the consecutive treatment throughout the entire differentiation process (Fig. 4A, 4B). When applied from day 6 to day 9, the EHMT inhibitors slightly increased platelet production (Fig. 4A, 4B). By contrast, little enhancement of MK and platelet generation was observed when UNC0631 or A366 was added during other stages (Fig. 4A, 4B). Thus, the transient treatment of EHMT inhibitors at the early proliferation stage is sufficient to achieve maximal enhancement of platelet generation.

We further assessed the functional integrity of platelets by measuring their capability of shape change and a-granule release. Expectedly, the platelets enriched from both groups were able to undergo normal shape change and to spread out after the stimulation by thrombin (Fig. 4C), highly reminiscent of platelets from peripheral blood.⁸ Furthermore, platelets from the EHMT inhibitor group expressed a level of CD62P from a-granules to the surface of platelets comparable with the DMSO group in response to agonists (Fig. 4D), indicating that EHMT inhibitors not only promote platelet production but also maintain the functional integrity of generated platelets. To determine the effect of EHMT inhibitors in vivo, we transplanted the CB-derived cells with or without UNC0631 treatment into immunodeficiency mice (Fig. 4E). As expected, UNC0631 ultimately augmented the proportion of human platelets in the peripheral blood of mice (Fig. 4F). Thus, early transient stimulation of CB-HSPCs with EHMT inhibitors also increases the final production of viable platelets in vivo.

EHMT Inhibitors Substantially Boost Platelet Production by Promoting Cell Proliferation

The pronounced stimulation of platelet production by UNC0631 or A366 at the early proliferative stage led us to speculate that EHMT inhibitors might enhance the proliferation and differentiation potential of HSPCs. Indeed, both UNC0631 and A366 caused strong effects on cell proliferation after 6 days of culture, while the effect became increasingly apparent with MK differentiation (Fig. 5A,

Supplementary Fig. S4A). The remarkable expansion of total cells also enhanced the final yield of platelets from a single CD34⁺ progenitor cell (Fig. 5B). The analysis of cell cycle progression showed that the percentage of BrdU⁺ cells, indicative of a highly proliferative state, was significantly elevated after UNC0631 treatment (Fig. 5C). Furthermore, after UNC0631 treatment cells gradually accumulated in the S phase of the cell cycle, while the proportion of cells in G0/G1 phase was significantly reduced (Fig. 5D), indicating a higher proliferative potential of cells with UNC0631 treatment.

To test the effects of EHMT inhibitors on thrombopoiesis, we further compared the maturation of MKs with or without EHMT inhibitor treatment. Surprisingly, no significant differences in cell size, ploidy, and the percentage of proplatelet-forming MKs were observed between the 2 groups (Supplementary Fig. S4B, S4D). The expression of CD148, a surface marker specifically expressed in mature MKs with elevated potency of polyploidization and thrombopoiesis,¹¹ also had no significant change after UNC0631 treatment (Supplementary Fig. S4E). Thus, the treatment with EHMT inhibitors led to a much higher yield of platelets in the culture, mainly by the promotion of cell proliferation, rather than the enhancement of the thrombopoiesis potential of MKs.

EHMT Inhibition Selectively Promotes the Expansion of Progenitor Cells in MK Lineage

To examine the effect of EHMT inhibitors on cell proliferation at the molecular level, we performed single-cell RNA-Seq of CB-derived cells with or without UNC0631 treatment. After the same quality control as described earlier was applied, 21 644 cells from 2 groups were selected for further analysis (Fig. 6A, Supplementary Fig. S5A). As expected, genes associated with “mitotic cell cycle” and “DNA-dependent DNA replication” showed higher expression in cells with UNC0631 treatment (Fig. 6B), which might result in G1 to S phase transition to enhance the proliferative potential of differentiated cells and lead to enhanced production of MKs and platelets.

To elucidate the potential mechanism by which EHMT inhibitors promote proliferation, we mapped the cell populations (depicted in Fig. 1B) into single cells with or without UNC0631 treatment, respectively (Fig. 6C). Interestingly, the fraction of cells in the predicted MEP population significantly increased after UNC0631 treatment (Fig. 6D). A moderate increase in MKP proportion was also observed in UNC0631-treated cells (Fig. 6D). In contrast, the non-MK progenitors, including iMP, EBMP, and NeuP populations, were dramatically reduced with UNC0631 addition (Fig. 6E). Furthermore, the genes in Module 1 identified in Fig. 1I exhibited higher expression in UNC0631-treated cells (Fig. 6F), probably contributing to the high proliferative potential of MK progenitors. When comparing the transcriptome of MKs from control and those after EHMT inhibition, no significant differences were observed in the expression of genes related to MK polyploidization and thrombopoiesis, such as *TUBB1* and *CD226* (Supplementary Fig. S5B–S5D), confirming that EHMT inhibition had little effect on MK maturation.

Therefore, EHMT inhibitors may induce the broad expression of cell cycle-related genes and the selective expansion of MEP and MKP populations, thus enabling long-term cell proliferation and the abundant production of MKs and platelets.

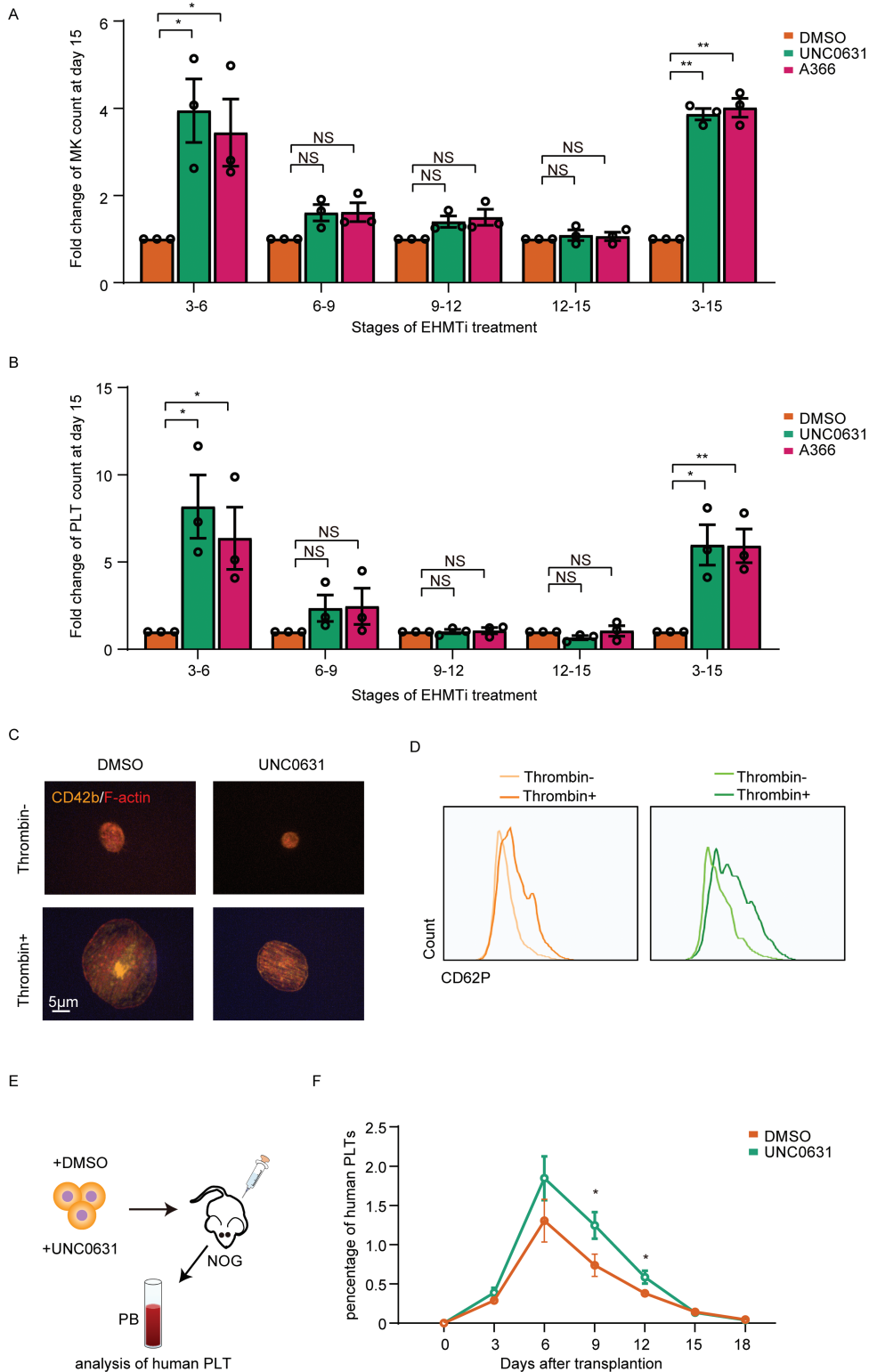


Figure 4. EHMT inhibitors exert their effects at the early proliferation stage. **(A)** Fold changes of MK count at day 15 after the treatment with UNC0631 and A366 at different time windows ($n = 3$). **(B)** Fold changes of platelet count at day 15 after the treatment with UNC0631 and A366 at different time windows ($n = 3$). **(C)** CD42b (yellow) and F-actin (phalloidin; red) staining of platelets in 2 groups bound to immobilized fibrinogen in the absence or presence of 1 U/mL thrombin (scale bar = 5 µm). **(D)** The representative histograms of P-selectin (CD62P) expression with or without thrombin stimulation analyzed by flow cytometry in platelets from 2 groups. **(E)** Schematic diagram of in vivo transplantation assay. **(F)** Percentage of human platelets in mouse peripheral blood at different time points after transplantation ($n = 5$). Abbreviations: EHMT, euchromatic histone lysine methyltransferase; MK, megakaryocyte. Student's t test, * $P < .05$, ** $P < .01$, and *** $P < .001$.

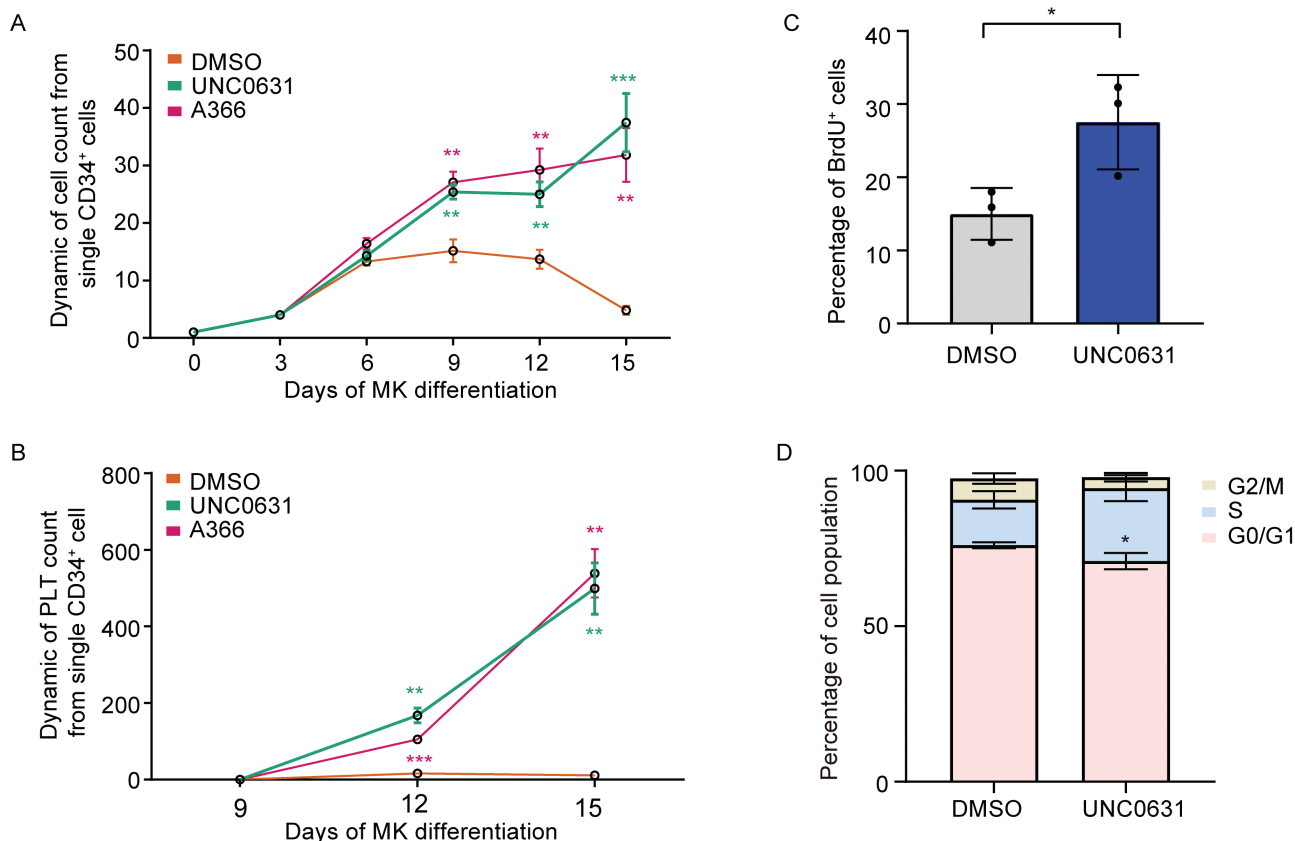


Figure 5. EHMT inhibitors substantially boost platelet production by promoting cell proliferation. **(A)** Dynamics of cell count from single CD34⁺ cells with DMSO, UNC0631, and A366 treatment ($n = 3$). **(B)** Dynamics of platelet count from single CD34⁺ cells with DMSO, UNC0631, and A366 treatment ($n = 3$). **(C)** Percentage of BrdU⁺ cells with DMSO and UNC0631 treatment during proliferation stage ($n = 3$). **(D)** Percentage of cells in G2/M, S, or G0/G1 phase with or without UNC0631 treatment ($n = 3$). Abbreviations: DMSO, dimethyl sulfoxide; EHMt, euchromatic histone lysine methyltransferase. Student's *t* test, * $P < .05$, ** $P < .01$, and *** $P < .001$.

Discussion

The results from our current study reveal, for the first time, the transcriptional landscape of human neonatal megakaryopoiesis, the cellular heterogeneity and distinct molecular characteristics of CB-derived MKs, and the regulatory network governing MK differentiation from MEPs to MKs via MKPs. Using the CB-based model, we identified EHMt inhibitors as powerful tools for substantial improvement of platelet production. These EHMt inhibitors selectively amplify progenitors in the MK lineage and endow cells with long-term proliferative capacity, the promotion effect of which is increasingly obvious along with MK differentiation, having great potential for future applications for large-scale generation of platelets.

Megakaryopoiesis is a complex process that starts in the third week of human development in the yolk sac (YS) and the subsequent fetal liver (FL),²² while investigations of adult MKs predominantly concentrate on the BM.²³ Accumulating evidence suggests that MKs exhibit clear developmental and functional heterogeneity.¹⁶ Our previous studies have unveiled the transcriptional heterogeneity of human embryonic and adult MKs both in vivo and in vitro.^{10,11} Interestingly, the MK subpopulation with thrombopoiesis and immune features present in adult MKs from BM are also present in embryonic MKs from YS and FL or hESCs,^{10,11} substantiating the nontraditional functions of MKs beyond platelet production. However, the molecular features of neonatal MKs were undefined by these earlier studies. In the current study, we

further modeled human megakaryopoiesis from CB-CD34⁺ cells and unveiled the cellular heterogeneity of neonatal MKs. By using comparative analyses, we found that the overall transcriptome characteristics of MKs and the classifications of cell subpopulations are closer to BM MKs. These data are consistent with the previously documented differences of MKs from different stem cell sources in cell size, DNA content, and platelet production.²⁴ Therefore, this study advances our understanding of human neonatal megakaryopoiesis and provides a comprehensive knowledge base for future studies.

It is well established that the process of megakaryopoiesis in vitro initiates with the enrichment and amplification of HSPCs, followed by MK differentiation of HSPCs and subsequent MK maturation through DNA polyploidization, cytoplasmic enlargement, proplatelet formation, and platelet release. Accordingly, the optimization of each of these steps, especially the progenitor amplification, might lead to the increase of the final yield of platelets. Among a variety of strategies, small molecules have the unique advantages of convenient operation and strong controllability and therefore have been widely used to improve the progenitor expansion and platelet generation from primary CD34⁺ cells. For example, StemRegenin 1 (SR1), an antagonist of the aryl hydrocarbon receptor transcription factor, is known to promote the expansion of human HSPCs²⁵ and leads to an enrichment of CD34⁺CD41^{low} megakaryocytic precursors with an increased capacity to generate mature MKs and platelets.²⁶ Our group also identified a combination of small molecules

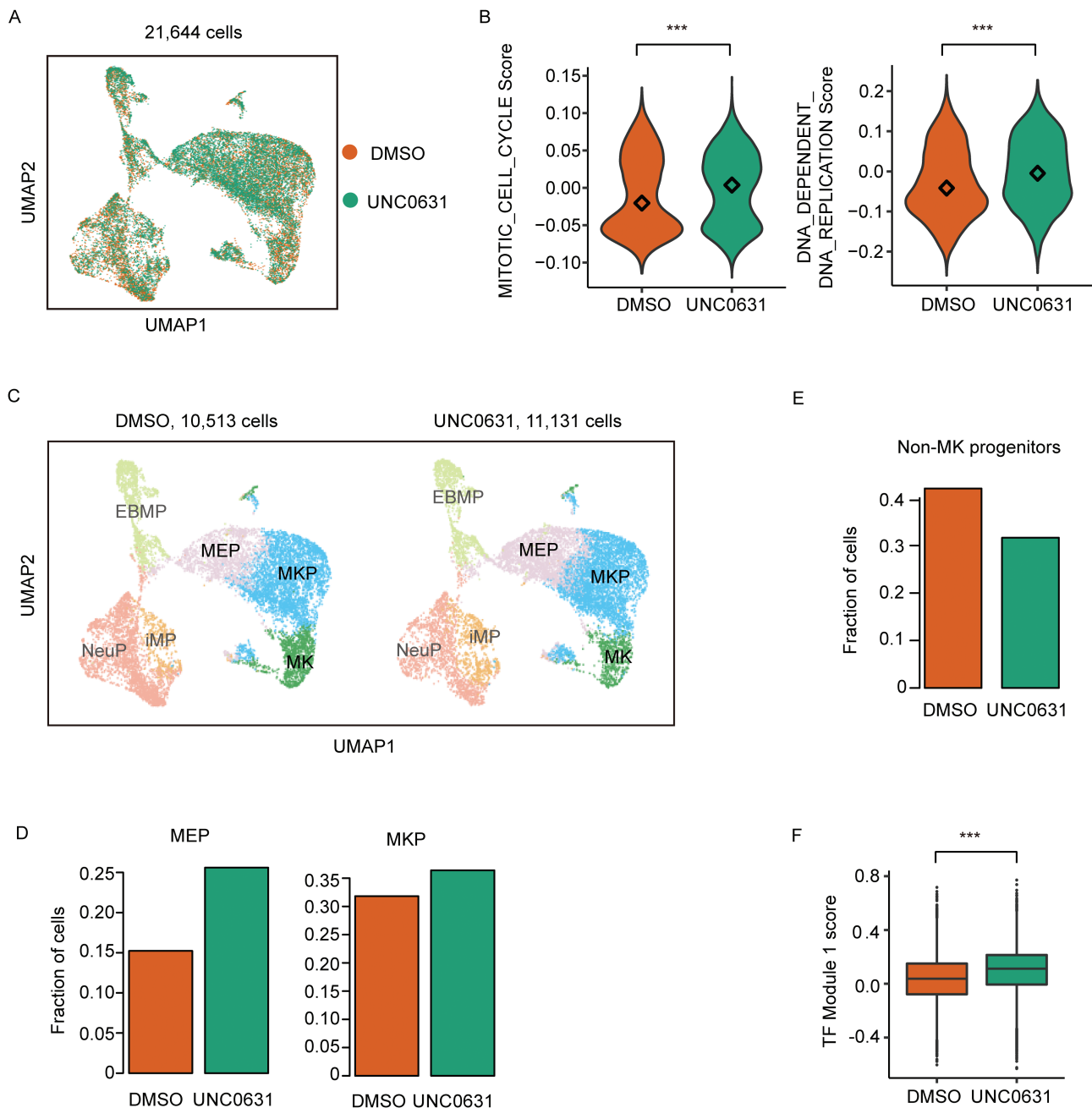


Figure 6. EHMT inhibition selectively promotes the expansion of progenitor cells in MK lineage. **(A)** UMAP showing CB-derived single cells with or without UNC0631 treatment. Colors indicate different groups. **(B)** The expression score of genes involving in mitotic cell cycle (left) and DNA replication (right) between DMSO and UNC0631 groups. Unpaired 2-sided Wilcoxon test, $***P < .001$. **(C)** UMAP showing CB-derived cells separated by experimental with predicted cell type based on Fig. 1B. **(D)** The fractions of MEPs and MKPs in the DMSO and UNC0631 groups. **(E)** The fraction of non-MK progenitors in DMSO and UNC0631 groups. **(F)** The expression score of significant TFs in Module 1 calculated in DMSO and UNC0631 groups. Unpaired 2-sided Wilcoxon test, $***P < .001$. Abbreviations: CB, cord blood; DMSO, dimethyl sulfoxide; EHMT, euchromatic histone methyltransferase; MEPs, megakaryocyte-erythroid progenitors; MK, megakaryocyte; MKPs, megakaryocyte progenitors; UMAP, Uniform Manifold Approximation and Projection.

via stage-specific screening, significantly promoting platelet production from CB-derived MKs.⁸ In the present study, we identified a class of small molecules, namely the EHMT inhibitors, which, when transiently applied at the early stage, can significantly enhance platelet production with nearly a 30-fold increase, thereby offering a powerful tool for in vitro platelet manufacture and clinical applications.

As a significant form of epigenetic regulation, histone methylation, catalyzed by a specific enzyme called

methyltransferase, plays a pivotal role in many biological and pathological processes.²⁷ The 2 compounds UNC0631 and A366 used in this study are histone methyltransferase inhibitors selectively targeting the euchromatic histone methyltransferase 2 (EHMT2), also termed as G9a.²⁸ By altering the function of H3K9 histones, G9a inhibitors are well-known agents regulating cell proliferation and cancer metastasis.²⁸ However, the function of G9a in human hematopoiesis is poorly investigated.

In this research, we uncovered, for the first time, the effect of G9a inhibitors UNC0631 and A366 on the expansion of progenitors in MK lineage, especially the MEP population. In addition, the EHMT inhibitors alter the transcription factor regulatory network during MK differentiation, enhance the proliferation of progenitor cells, and consequently generate a large number of MKs and platelets. However, the promotion effects on proliferation induced by EHMT2 knockdown, which is also observed decreased the H3K9me2 level, is not as significantly as EHMT inhibitors. We speculate that the effect of EHMT inhibitors should be only partially due to the methyltransferase activity. A more detailed delineation of the molecular mechanism underlying the action of EHMT inhibitors awaits future experimentation. Also, the much more moderate effects of EHMT inhibitors *in vivo* were observed, and the underlying mechanism also needs to be further explored.

Overall, our study utilizing single-cell transcriptomic analysis of various developmental models has broadened the knowledge of megakaryopoiesis and thrombopoiesis under both physiological and pathological conditions and revealed a new strategy to improve platelet production from readily available progenitor sources. Furthermore, the combined use of potent chemical compounds and bioreactors should significantly improve the derivation of functional platelets *in vitro* from stem cells and thereby facilitate the use of platelets for transfusion and other clinical applications.

Funding

This work was supported by the National Natural Science Foundation of China (82125003, 81870099), the National Key Research and Development Program of China (2021YFA1103000, 2021YFA1100703), the CAMS Innovation Fund for Medical Sciences (2021-I2M-1-073), the Non-profit Central Research Institute Fund of Chinese Academy of Medical Sciences (2021-RC310-019), and Cooperation Project of Beijing-Tianjin-Hebei Basic Research (19JCZDJC65700(Z)).

Conflict of Interest

The authors declared no potential conflicts of interest.

Author Contributions

Y.L.: performed experiments and data collection; Y.L. and C.L.: carried out the single-cell RNA-Seq analysis; J.Z.: carried out the single-cell RNA-Seq analysis; Y.W.: provided small molecules; H.W. and P.S.: provided new thoughts; C.L. and J.Z.: project design, wrote and edited manuscript.

Supplementary Material

Supplementary material is available at *Stem Cells Translational Medicine* online.

References

- Xu XR, Zhang D, Oswald BE, et al. Platelets are versatile cells: new discoveries in hemostasis, thrombosis, immune responses, tumor metastasis and beyond. *Crit Rev Clin Lab Sci*. 2016;53(6):409-430. <https://doi.org/10.1080/10408363.2016.1200008>
- Kumar A, Mhaskar R, Grossman BJ, et al. AABB Platelet Transfusion Guidelines Panel. Platelet transfusion: a systematic review of the clinical evidence. *Transfusion*. 2015;55(5):1116-1127; quiz 1115. <https://doi.org/10.1111/trf.12943>
- Garraud O. How do I see the production of engineered blood cells available for transfusion? *Transfus Apher Sci*. 2020;59(4):102863. <https://doi.org/10.1016/j.transci.2020.102863>
- Levy JH, Neal MD, Herman JH. Bacterial contamination of platelets for transfusion: strategies for prevention. *Crit Care*. 2018;22(1):271. <https://doi.org/10.1186/s13054-018-2212-9>
- Proder CF, Rampotas A, Estcourt LJ, Stanworth SJ, Murphy MF. Platelet transfusion: alloimmunization and refractoriness. *Semin Hematol*. 2020;57(2):92-99. <https://doi.org/10.1053/j.seminhematol.2019.10.001>
- Reems JA, Pineault N, Sun S. *In vitro* megakaryocyte production and platelet biogenesis: state of the art. *Transfus Med Rev*. 2010;24(1):33-43. <https://doi.org/10.1016/j.tmr.2009.09.003>
- Orlando N, Pellegrino C, Valentini CG, et al. Umbilical cord blood: current uses for transfusion and regenerative medicine. *Transfus Apher Sci*. 2020;59(5):102952. <https://doi.org/10.1016/j.transci.2020.102952>
- Yang Y, Liu C, Lei X, et al. Integrated biophysical and biochemical signals augment megakaryopoiesis and thrombopoiesis in a three-dimensional rotary culture system. *Stem Cells Transl Med*. 2016;5(2):175-185. <https://doi.org/10.5966/sctm.2015-0080>
- Perdomo J, Yan F, Leung HHL, Chong BH. Megakaryocyte differentiation and platelet formation from human cord blood-derived CD34⁺ cells. *J Vis Exp*. 2017;(130):56420. <https://doi.org/10.3791/56420>
- Wang H, He J, Xu C, et al. Decoding human megakaryocyte development. *Cell Stem Cell*. 2021;28(3):535-549.e8. <https://doi.org/10.1016/j.stem.2020.11.006>
- Liu C, Wu D, Xia M, et al. Characterization of cellular heterogeneity and an immune subpopulation of human megakaryocytes. *Adv Sci (Weinh)*. 2021;8(15):e2100921. <https://doi.org/10.1002/adv.202100921>
- Velten L, Haas SF, Raffel S, et al. Human haematopoietic stem cell lineage commitment is a continuous process. *Nat Cell Biol*. 2017;19(4):271-281. <https://doi.org/10.1038/ncb3493>
- Hongtao W, Cuicui L, Xin L, et al. MEIS1 regulates hemogenic endothelial generation, megakaryopoiesis and thrombopoiesis in human pluripotent stem cells by targeting TAL1 and FLI1. *Stem Cell Rep*. 2018;10(2):447-460.
- Pang L, Xue HH, Szalai G, et al. Maturation stage-specific regulation of megakaryopoiesis by pointed-domain Ets proteins. *Blood*. 2006;108(7):2198-2206. <https://doi.org/10.1182/blood-2006-04-019760>
- Elagib KE, Brock AT, Goldfarb AN. Megakaryocyte ontogeny: clinical and molecular significance. *Exp Hematol*. 2018;61:1-9. <https://doi.org/10.1016/j.exphem.2018.02.003>
- Liu C, Huang B, Wang H, Zhou J. The heterogeneity of megakaryocytes and platelets and implications for *ex vivo* platelet generation. *Stem Cells Transl Med*. 2021;10(12):1614-1620. <https://doi.org/10.1002/sctm.21-0264>
- Hamilton S, de Cabo R, Bernier M. Maternally expressed gene 3 in metabolic programming. *Biochim Biophys Acta Gene Regul Mech*. 2020;1863(4):194396. <https://doi.org/10.1016/j.bbagr.2019.06.007>
- Xie X, Liu M, Zhang Y, et al. Single-cell transcriptomic landscape of human blood cells. *Natl Sci Rev*. 2020;8(3). <https://doi.org/10.1093/nsr/nwaa180>
- Seo H, Chen SJ, Hashimoto K, et al. A β 1-tubulin-based megakaryocyte maturation reporter system identifies novel drugs that promote platelet production. *Blood Adv*. 2018;2(17):2262-2272. <https://doi.org/10.1182/bloodadvances.2018019547>
- Liu F, Baryte-Lovejoy D, Allali-Hassani A, et al. Optimization of cellular activity of G9a inhibitors 7-aminoalkoxy-quinazolines. *J Med Chem*. 2011;54(17):6139-6150. <https://doi.org/10.1021/jm200903z>

21. Sweis RF, Pliushchev M, Brown PJ, et al. Discovery and development of potent and selective inhibitors of histone methyltransferase G9a. *ACS Med Chem Lett.* 2014;5(2):205-209. <https://doi.org/10.1021/ml400496h>
22. Palis J. Hematopoietic stem cell-independent hematopoiesis: emergence of erythroid, megakaryocyte, and myeloid potential in the mammalian embryo. *FEBS Lett.* 2016;590(22):3965-3974. <https://doi.org/10.1002/1873-3468.12459>
23. Machlus KR, Italiano JE Jr. The incredible journey: from megakaryocyte development to platelet formation. *J Cell Biol.* 2013;201(6):785-796. <https://doi.org/10.1083/jcb.201304054>
24. Bluteau O, Langlois T, Rivera-Munoz P, et al. Developmental changes in human megakaryopoiesis. *J Thromb Haemost.* 2013;11(9):1730-1741. <https://doi.org/10.1111/jth.12326>
25. Tao L, Togarrati PP, Choi KD, Suknuntha K. StemRegenin 1 selectively promotes expansion of multipotent hematopoietic progenitors derived from human embryonic stem cells. *J Stem Cells Regen Med.* 2017;13(2):75-79.
26. Strassel C, Brouard N, Mallo L, et al. Aryl hydrocarbon receptor-dependent enrichment of a megakaryocytic precursor with a high potential to produce proplatelets. *Blood.* 2016;127(18):2231-2240. <https://doi.org/10.1182/blood-2015-09-670208>
27. Zhang Y, Sun Z, Jia J, et al. Overview of histone modification. *Adv Exp Med Biol.* 2021;1283:1-16. https://doi.org/10.1007/978-981-15-8104-5_1
28. Cao H, Li L, Yang D, et al. Recent progress in histone methyltransferase (G9a) inhibitors as anticancer agents. *Eur J Med Chem.* 2019;179:537-546. <https://doi.org/10.1016/j.ejmech.2019.06.072>